ISSN:2617-4294

المجلة العلمية لكلية التربية

مجلة علمية نصف سنوية محكمة

تصدر عن كلية التربية - جامعة ذمار

المجلة العلمية لكلية التربية

مجلة علمية نصف سنوية

تعنى بالدراسات والبحوث الإنسانية والعلمية المختلفة ـ تصدر عن كلية التربية ـ جامعة ذمار

جميع البحوث تعبر عن آراء أصحابها،
ولا تعبر بالضرورة عن رأي المجلة

المجلة العلمية لكلية التربية

تعنى بالدراسات والبحوث الإنسانية والعلمية المختلفة

تصدر عن كلية التربية

جامعة ذمار

الجمهورية اليمنية

العدد: التاسع عشر

أكتوبر 2023

الترقيم الدولي:

(ISSN: 2617-4294)

(DOI: 10.60037)

الترقيم المحلي:

2006/129

قواعد النشر

المجلة العلمية لكلية التربية هي مجلة علمية نصف سنوية، تصدر عن كلية التربية – جامعة ذمار، الجمهورية اليمنية، تحمل الرقم الدولي الآتي: (ISSN: 2617-4294). وتعنى بالدراسات والبحوث الإنسانية والعلمية المختلفة، باللغات العربية، والإنجليزية، وتقبل نشر البحوث وفقًا لقواعد النشر الآتية:

- أن تتسم الأبحاث بالأصالة والمنهجية العلمية السليمة.
- أن لا يكون البحث قد سبق نشره، أو إرساله للنشر إلى جهة أخرى، ويقدم الباحث إقرارا خطيًّا عن ذلك.
- يكتب البحث بلغة سليمة، ويراعى فيه قواعد الضبط ودقة الأشكال -إن وجدت- في صيغة Word ويكتب البحث بخط Sakkal Majalla وحجم 15 بالنسبة إلى الأبحاث باللغة العربية، وهوامش بحجم11، وخط Sakkal Majalla للبحوث بالإنجليزية وحجم 14، وهوامش بحجم12، وتكون العناوين الرئيسة بخط غامق، و حجم14، على أن تكون المسافة بين الأسطر 1 سم، ومسافة الهوامش 2,5سم من كل جانب.
- لا يتجاوز البحث 10000 كلمة، ولا يقل عن 6000 كلمة، بما فيها الأشكال والجداول والملاحق.
- يتجنب الباحث الانتحال أو اقتباس أفكارهم الآخرين وآراءهم دون الإشارة إلى مصادرها الأصلية.

ثانيا: إجراءات التقديم للنشر:

يلتزم الباحث بترتيب البحث وفق الخطوات الآتية:

- يقوم الباحث بتصفيف بحثه في نموذج المجلة word، بتنزيله من موقع الجامعة قسم المجلات العلمية رابط:

  https://www.tu.edu.ye/ أو طلبه عبر إيميل المجلة: journal_sei_edu2006@tu.edu.ye

- تحتوي الصفحة الأولى على بيانات البحث والباحث يكتب فيها العنوان بالعربية واسم الباحث ووصفه الوظيفي، والمؤسسة التي ينتمي إليها، وبريده الإلكتروني، وترجمة كل ذلك إلى الإنجليزية، ثم ملخص البحث في عمودين: الأول: عربي ، والعمود الثاني ترجمة إلى اللغة الإنجليزية لمحتويات العمود الأول، والكلمات المفتاحية.

- يوضح الباحث هدف البحث، والمنهجية، وأهم نتيجة في الملخص (على ألا يزيد الملخصان بالعربية والإنجليزية، كل منهما عن170 كلمة، ولا يقل عن 120 كلمة، في فقرة واحدة، ويرفق معهما كلمات مفتاحية بحيث لا تزيد عن 6 كلمات.

- **المقدمة**: يحتوي البحث على مقدمة يستعرض فيها الباحث: نبذة عن الموضوع، الدراسات السابقة، ثم الجديد الذي سيضيفه البحث في مجاله، إشكالية البحث، أهدافه، أهميته، ومنهجه، وخطة سيره في بحثه، بشكل مترابط ومتسلسل.
- النتائج: يتم عرض النتائج بشكل واضح ودقيق.
- الهوامش والمراجع: توثق الهوامش في نهاية الأبحاث حسب الآتي:
- يبدأ الباحث في الهوامش بكتابة لقب المؤلف، ثم اسمه العلم، ثم عام الطبع، ثم عنوان البحث/الكتاب مختصرا، دار النشر، مكان الطبع، ومن ثم الجزء إن وجد، وإذا لم يجد جزءا يكتب رقم الصفحة مباشرة، مثلا: المقري، 2009، نفح الطيب، دار الكتب العلمية-بيروت، ص: 1. وسوسير،2022، علم اللغة العام، عالم الكتب- عمّان، ص: 100.
- يتم ترتيب المصادر والمراجع ألفبائيًّا، على أن لا يدخل في الترتيب أل، وأبو، وابن، فابن منظور مثلا يرتب في حرف الميم.
- ترسل الأبحاث باسم رئيس التحرير على البريد الإلكتروني المحدد للمجلة PDF & و Word journal_sei_edu2006@tu.edu.ye
- تتولى هيئة تحرير المجلة إبلاغ الباحث باستلام بحثه، وإجازته للتحكيم، أو التعديل عليه قبل إجازته للتحكيم.
- تقوم هيئة تحرير المجلة برومنة المراجع وتنسيقها بعد اعتمادها وتدقيقها في شكلها النهائي.
- يجوز لهيئة تحرير المجلة تعديل أي نص في البحوث بما يتوافق مع المراجعات اللغوية.

ثالثا: إجراءات التحكيم والنشر:

- بعد إجازة البحث للتحكيم من قبل رئيس التحرير، أو مدير التحرير تتم إحالته للتحكيم.
- تخضع الأبحاث المقدمة للنشر في المجلة العلمية للتحكيم العلمي من قبل محكمين متخصصين.
- يصدر قرار قبول البحث بالنشر من عدمه بناء على التقارير المقدمة من المحكمين.
- تتولى هيئة تحرير المجلة إبلاغ الباحث بقرار المحكمين حول صلاحيته للنشر من عدمه، أو إجراء التعديلات الموصى بها.

-يلتزم الباحث بالتعديلات التي يوصي بها المحكمون في البحث وفقًا لاستمارة التحكيم المرسلة إليه، في أقرب أجل ممكن.

-يعاد البحث إلى المحكمين عندما تكون التوصيات جوهرية؛ لمعرفة مدى التزام الباحث بذلك.

-تتولى هيئة تحرير المجلة متابعة التقييم عندما تكون التوصية بإجراء تعديلات طفيفة، ومن ثم يتم

التحقّق النهائيّ، ويُمنح الباحث خطاب قبول بالنشر، متضمنا رقم العدد الذي سوف ينشر فيه وتاريخه.

-بعد التأكد من جاهزية المخطوطة بصورتها النهائية، يتم إرسالها إلى التدقيق اللغوي والمراجعة الفنية، ثم تحال إلى الإنتاج النهائي.

- يعاد البحث بصورته النهائية إلى الباحث قبل النشر للمراجعة النهائية وإبداء الملاحظات إن وجدت، وفق النموذج المعدّ لذلك.

- يتم نشر الأعداد إلكترونيًّا في موقع المجلة، وترسل ورقيا لمن أراد من كل عدد وفق الخطة الزمنية المحددة للنشر، ويتاح تحميلها مجانا على الرابط الآتي:https://www.tu.edu.ye/journals/index.php/edu

رابعا: أجور النشر:

يدفع الباحثون الأجر المقرر حسب الآتي:

- يدفع أعضاء هيئة التدريس في جامعة ذمار مبلغ 20000 ألف ريال يمني.

- يدفع الباحثون اليمنيون من داخل اليمن 30000ألف ريال يمني.

- يدفع الباحثون من خارج اليمن100 دولارًا أمريكيًّا أو ما يعادلها.

-يدفع الباحث مقدما أجور إرسال النسخ الورقية من العدد إن أراد نسخة ورقية.

- لا يعاد المبلغ في حالة رُفض البحث من قبل المحكمين.

للاطلاع على الأعداد السابقة يرجى زيارة موقع المجلة عبر الرابط:

https://www.tu.edu.ye/journals/index.php/edu

- **المراسلات على العنوان البريدي والإلكتروني الآتي:** journal_sei_edu2006@tu.edu.ye

عنوان المجلة:

كلية التربية – جامعة ذمار – ص ب: (87246) ت: (06509121 - 06509132) فاكس: (06509556).

Faculty of Education, Thamar University - P.O.Box: (06509121 - 06509132) Fax: (06509556).

http://tu.edu.ye/faculty/education/ - E-mail: journal_sei_edu2006@tu.edu.ye

المحتويات

الصفحات: 382- 399

العدد 19 - أكتوبر 2023
Issue 19– Oct 2023
The Scientific Journal of the Faculty of Education

Structural, Optical, and Electrical Properties of Pure α-Al_2O_3 Nanopowders with Add V_2O_7 and Cu_2O by Sol-Gel Method

الخواص التركيبية والضوئية والكهربائية لمساحيق α-Al2O3 النانوية النقية مع إضافة V2O7 و Cu2O بطريقة السوجل

S. Al-Ariki سامي. العريقي
Department of Physics, College of Education, Dhamar University – Yemen

قسم الفيزياء، كلية التربية جامعة ذمار- اليمن.

M. A. Ali. AL-Mushaki محمد علي الموشكي
Shakib Moqbel Alsowidy شكيب مقبل السويدي
Department of Physics, College of Science, Sana'a University – Yemen

قسم الفيزياء، كلية العلوم، جامعة صنعاء- اليمن
samimukred@gmail.com

تاريخ الاستلام: 2023/10/12 تاريخ القبول: 2023/10/20 تاريخ النشر: 2023/10/30

Abstract

This manuscript explored the synthesis and comprehensive characterization of pure α-Al_2O_3 and (α-Al_2O_3)$_{8-x}$(V_2O_7)$_{20}$(Cu_2O)$_x$ at varying molar ratios (x = 1%, 2%, and 3%) in nanopowder form, prepared using the sol-gel method. After subjecting the samples to heat treatment, X-ray diffraction (XRD) revealed their high crystallinity. The crystallite size was calculated using the Scherrer formula, exhibited variations among the samples with pure α-Al_2O_3 possessing a size of 43.10 nm and the mixed oxide nanopowders falling within the range of 29.54 nm to 34.84 nm. These materials displayed semiconductor characteristics, with band gap values ranging from 3.28 eV to 5.21 eV. Moreover, as the molar concentration of copper increased, electrical conductivity improved, signifying potential applications in systems requiring regulated electrical behavior. These findings highlight the versatility of these materials, offering opportunities for tailored crystallinity, band gap tuning, and controlled electrical properties, making them suitable for diverse technological and scientific applications.

Keywords: Structural, Optical, and Electrical Properties; α-Al_2O_3/VO/CuO; nanopowders

ملخص البحث:

يهدف هذا البحث إلى بيان التوليف والتوصيف الشامل لـ α-Al2O3النقي و α-Al2O3)8-x(V2O7)20(Cu2O)xبنسب مولية متفاوتة(x = 1% ، 2%، و3%) في شكل مسحوق نانوي تم تحضيره بطريقة السول جل. وبعد إخضاع العينات للمعالجة الحرارية، اكتشفنا تحييد الأشعة السينية (XRD) عن درجة تبلورها العالية. وتم حساب الحجم البلوري باستخدام صيغة شيرل، وأظهرت اختلافات بين العينات ذات α-Al2O3 النقي الذي يمتلك حجم 43.10 نانومتر ومساحيق الأكسيد النانوية المختلطة التي تقع في نطاق 29.54 نانومتر إلى 34.84 نانومتر. وأظهرت هذه المواد خصائص أشباه الموصلات، إذ تتراوح قيم فجوة النطاق من 3.28 فولت إلى 5.21 فولت. علاوة على ذلك، مع زيادة التركيز المولي للنحاس، تحسنت الموصلية الكهربائية، مما يدل على التطبيقات المحتملة في الأنظمة التي تتطلب سلوكًا كهربائيًا منظمًا. وأهم نتائج البحث تتمثل في تسلط الضوء على تنوع هذه المواد، مما يوفر فرصًا لبلورة مخصصة، وضبط فجوة النطاق، والخواص الكهربائية الخاضعة للتحكم، ليجعلها مناسبة للتطبيقات التكنولوجية والعلمية المتنوعة.

الكلمات المفتاحية: الخصائص الهيكلية والبصرية والكهربائية α-Al2O3/VO/Cu؛ مساحيق النانو.

1. Introduction

Metal oxide nanoparticles have gained widespread prominence due to their remarkable properties and their myriad applications in both optical and electrical fields [1]. Among these metal oxides, aluminum oxide (Al_2O_3) stands out as a versatile ceramic material extensively employed in various applications, including catalysts, transparent armor for ballistic instruments, lasers, discharge lamps, and infrared (IR) airborne sensors [2]. Notably, Al_2O_3 exists in multiple structural forms, denoted by symbols like α, κ, ɵ, γ, β, χ, δ, and ή [3]. Among these, α-alumina oxide (α-Al_2O_3 or corundum) holds a distinguished place due to its thermodynamic stability and finds applications in transparent armor for ballistic protection, ceramics, high-strength materials, adsorbents, catalysts, catalyst supports, high-performance field-effect transistors (FETs), electrical insulators, optoelectronics, thermoluminescent dosimeters, lasers, light-emitting displays, cutting tools, spark plugs, and gas sensing [2,4-6].

α-Al_2O_3 forms when exposed to temperatures above 1100 °C, adopting a hexagonal crystalline structure with lattice parameters a=4.758 and c=12.991 [1,7]. This phase exhibits a direct energy transition and energy gap (E_g) ranging from 4.116 to 8.8 eV [4,8]. Despite its excellent thermal properties, α-Al_2O_3 is less favorable in terms of optical and electrical characteristics. However, a previous study [1] has shown that blending α-Al_2O_3 with V_2O_5 and CuO can enhance its structural properties while reducing the energy gap (Eg) and improving its electrical properties. Mixed oxide nanopowders containing α-Al_2O_3, V_2O_5, and CuO have found applications in diverse fields.

Among the vanadium oxide phases, V_2O_5 is the most stable and possesses a high oxidation state. Its distinctive structural properties make it valuable for applications such as solar cells, gas sensors, optical-electrical switches, chemical sensing, and electrochromic optoelectronic devices [9]. V2O5 has a direct energy gap (Eg) ranging from 2.2 to 2.8 eV, and it crystallizes in orthorhombic and tetragonal structures with lattice parameters a=3.561, b=11.501, and c=4.378 [4,10].

Copper oxide (CuO) is a p-type semiconductor with a relatively small energy gap (Eg) ranging from 1.2 to 1.9 eV. It adopts a monoclinic

crystalline structure with lattice parameters a=4.69, b=3.42, and c=5.13 [11]. Research in this area has predominantly focused on nanomaterials with enhanced structural, optical, and electrical properties, synthesized through various methods such as sol-gel [4,1], hydrothermal [12], co-laser vaporization [3], and physical vapor deposition (PVD) [13].

In this study, we employ the sol-gel method to synthesize pure α-Al_2O_3 and $(\alpha\text{-}Al_2O_3)_{8-x}(V_2O_7)_2(Cu_2O)_x$ with x values of 1%, 2%, and 3%. Our investigation delves into the crystallinity size, optical properties, and electrical characteristics of these α-aluminum oxide nanopowders with different molar ratios. The aim is to harness the exceptional properties of aluminum oxide while incorporating V_2O_5 and CuO to enhance its optical and electrical attributes. Ultimately, this research explores the potential for tailored aluminum oxide materials that can find applications in various fields.

2. Experimental details

2.1. Materials

In this study, various materials were employed, including aluminum nitrate (Al $(NO_3)_3{\cdot}9H_2O$) (HIMEDIA, 95%), copper nitrate rehydrate (Cu $(NO_3)_2{\cdot}3H_2O$) (HIMEDIA, 99%), ethanol (C_2H_5OH) (SEGMA, 96%), and ammonium monodentate (NH_4VO_3) (HIMEDIA, 95%).

2.2. Synthesis method

The nanopowders of pure α-Al_2O_3 and $(\alpha\text{-}Al2O_3)_{80-x}(V_2O_7)_{20}(Cu_2O)_x$ with x values of 1%, 2%, and 3% were synthesized using the sol-gel method, as outlined below.

2.2.1. Synthesis pure α-Al_2O_3

To prepare pure α-Al_2O_3, 15g of Al $(NO_3)_3{\cdot}9H_2O$ was dissolved in 40 ml of ethanol to achieve a 1M solution at room temperature. The solution was stirred using a magnetic stirrer for 20 minutes until it became homogeneous. The temperature was then increased to 80 °C while maintaining continuous stirring, resulting in the formation of a gel solution. This solution was left in the beaker for 24 hours and subsequently dried in an oven at 180 °C for 2 hours. The resulting material was ground until it reached a soft powder consistency.

2.2.2. Synthesis $(\alpha\text{-}Al_2O_3)_{80-x}(V_2O_7)_{20}(Cu_2O)_x$

For the synthesis of $(\alpha\text{-}Al_2O_3)_{80-x}(V_2O_7)_{20}(Cu_2O)_x$, 10.50g of Al (NO3)3·9H2O was dissolved in 40 ml of ethanol to create a 0.7M solution at room temperature. Simultaneously, 935.8mg of ammonium monovanadate (NH_4VO3) was dissolved in 40 ml of ethanol to produce a 0.2M solution, and 966.4mg of $Cu(NO_3)_2$·3H2O was dissolved in 40 ml of ethanol to achieve a 0.1M solution. All these solutions were stirred with a magnetic stirrer for 20 minutes until they reached homogeneity. The homogeneous solutions were mixed together while stirring for 20 minutes at room temperature until a uniform solution formed. This mixture was then stirred for an additional 20 minutes at 80 °C to produce a gel, which was left in a beaker for 24 hours. Afterward, the gel was dried in an oven at 180 °C for 2 hours.

All samples underwent calcination at 1200 °C for 5 hours, and pellets for electrical measurements were prepared. The pellets were made using a pressing machine (Carver) under a pressure of 6000 kg, resulting in pellets with a diameter (d) of 13 mm and a thickness (L) of 2 mm.

2.3. Characterizations

The structural properties of the samples were assessed through X-ray diffraction (XRD) using a Shimadzu model 6100-EDX-720 with CuKα radiation at 1.54065 Å. XRD patterns were obtained in the angular range of 0–80°. The optical properties of the samples were examined using a UV-Vis spectrophotometer, specifically the Hitachi U3900 model.

3. Results and discussion

3.1. Structure Properties

In the analysis of the structural properties, we began with the examination of pure α-Al2O3, which exhibited characteristic X-ray diffraction (XRD) patterns, as illustrated in Figure 1. A series of distinct diffraction peaks of $\alpha\text{-}Al_2O_3$ were identified at 2θ angles of 25.50°, 35.20°, 37.70°, 43.30°, 52.60°, 57.46°, 61.30°, 66.50°, and 68.20°. These peaks corresponded to the atomic planes of (012), (104), (110), (113), (024), (116), (018), (214), and (300), respectively. The XRD pattern for pure α-Al2O3 closely matched the hexagonal crystal structure with space group R-

3c, consistent with standard JCPDS cards, No. 00-46-1212 and PDF #10-0173.

In the second sample, where the molar concentration of aluminum was reduced to 80% by the introduction of 20% vanadium, the intensity of XRD peaks for α-Al_2O_3 diminished, as depicted in Figure 1. This decrease in α-Al_2O_3 intensity can be attributed to the inclusion of impurity material V_2O_5, potentially leading to crystal disorder and deformation within pure α-Al_2O_3. Notably, new peaks emerged, indicating the presence of V_2O_5. These new peaks corresponded to standard reflection patterns in JCPDS card No. 00-45-1074 and PDF #41-1426, and they were observed at 2θ angles of 12.10°, 26.20°, 27.80°, and 28.80°, aligning with the (200), (330), (240), and (241) planes of V_2O_5, respectively.

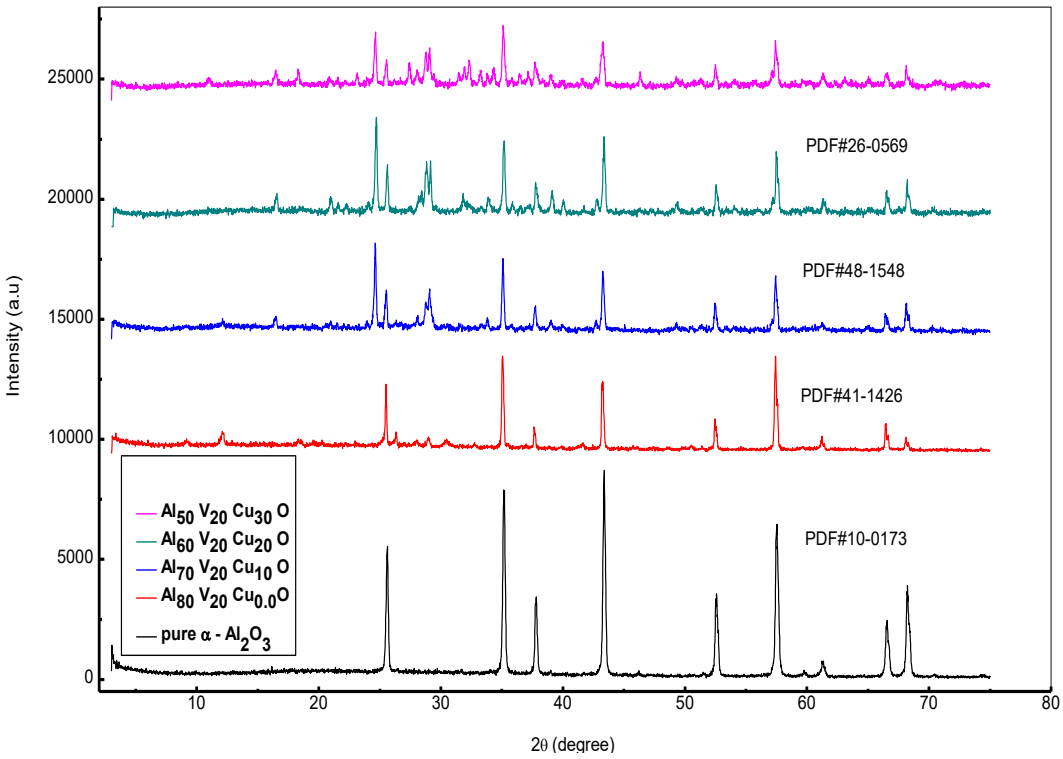

Fig 1. *XRD pattern a high crystallization nanopowders of pure α-Al_2O_3 and (α-Al_2O_3)$_{80-x}$ (V_2O_7)$_{20}$(Cu_2O)$_x$ at x = (1,2 and 3 %).*

In the third sample, the molar concentration of aluminum was further reduced to 70%, while introducing a 10% molar concentration of copper

while keeping the vanadium concentration consistent. The XRD patterns displayed a similar trend, with diminished α-Al2O3 intensity attributed to the introduction of CuO as an impurity, resulting in weak crystallinity. The CuO peaks were not distinct due to their weak crystalline nature. The 2θ values of 12.1°, 20.3°, 26.2°, and 39.9° aligned with (001), (110), (111), and (311) planes, respectively, and corresponded to JCPDS card No. 00-41-1426 and JCPDS card No. 00-26-0569. Furthermore, at 2θ values of 16.30°, 20.70°, 21.50°, 24.45°, 27.30°, 32.0°, 35.70°, 43.26°, and 49.30°, new peaks were observed, corresponding to (110), (111), (-112), (200), (112), (-133), (-221), (-131), and (133) crystalline planes of β-$Cu_2V_2O_7$. This formation was a result of thermal solid–solid interactions between copper and vanadium oxide phases in the mixed oxide nanopowders [2].

In the fourth sample, the molar concentration of copper was increased while decreasing the molar concentration of aluminum to 60%. This alteration led to an increase in the intensity of β-$Cu_2V_2O_7$ peaks, indicating improved crystallinity. Additionally, a new peak of CuO was observed at 2θ values of 38.90°, corresponding to (200) planes. This finding was consistent with the standard JCPDS card No. 00-48-1548. Furthermore, the CuO peak appeared at 2θ values of 61.30°, corresponding to the (-113) plane, and aligned with JCPDS card No. 00-045-0937 and PDF#26-0569, confirming its presence as per prior research [3,4]. In the fifth sample, with an increased molar concentration of copper up to 30%, new peaks were observed, indicating a further change in the crystalline structure.

The crystallite size of $(Al_2O_3)_{80-x}(V_2O_7)_{20}$ $(Cu_2O)_x$ at x = (1, 2, and 3%) was calculated using the Scherrer equation from Full Width Half Maximum (FWHM), as outlined in Equation.

$$D = \frac{0.89\,\lambda}{\beta\,\cos\theta} \qquad (1)$$

Where λ represents the wavelength of the X-ray, θ indicates Bragg's angle, and β shows the FWHM. The results are summarized in Table 1. It was observed that the crystallite size gradually decreased as the molar concentration of copper increased, transitioning from (43.10 nm) for pure α-Al2O3 to (29.54 nm) for (Al2O3)80-x (V2O7)20 (Cu2O) x at x = (1, 2, and 3%) in mixed oxide nanopowders, as presented in Figure 2. This decrease can be attributed to the fact that the ionic radius of aluminum oxide (0.54 Å)

is smaller than that of copper oxide (0.67 Å) and vanadium oxide (0.78 Å). Interestingly, the crystallite size of α-Al2O3 also decreased as the molar concentration of copper increased, indicating that the secondary phase's evolution influenced the particle size of the parent phase (α-Al2O3) during crystallization. These results align well with prior research [5].

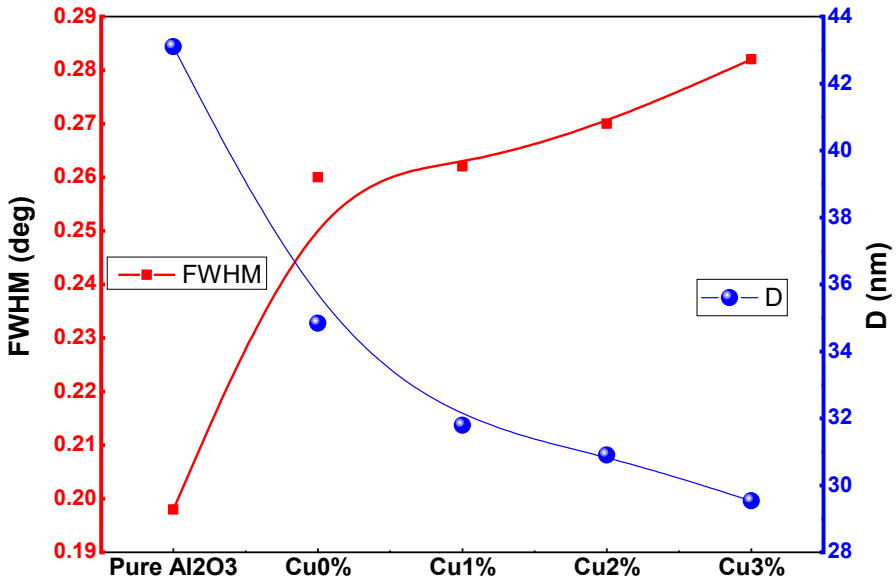

Fig 2 *Variation of full-width-at-half-maximum and crystallite sizes.*

Table 1 pure α-Al_2O_3 and $(Al_2O_3)_{80-x}(V_2O_7)_{20}(Cu_2O)_x$ at x = (1, 2 and 3 %) Nanopowders with were synthesized by sol-gel method.

Samples	Phase oxide	2θ (deg)	hkl	FWHM (deg)	d (Å)		a(Å)	c(Å)
					Expt	Std		
Pure α-Al_2O_3	α-Al2O3	43.30	113	0.198	2.085	2.085	4.756	12.993
$Al_{80}V_{20}Cu_{0.0}O$	α-Al_2O_3	57.00	116	0.260	1.601	1.601	4.117	13.021
$Al_{70}V_{20}Cu_{10}O$	α-Al_2O_3	35.00	104	0.262	2.561	2.550	4.115	13.002
	β-	24.46	200	0.528	3.636	3.600	7.330	10.20

	Cu2V2O7							0
$Al_{60}V_{20}Cu_{20}O$	α-Al_2O_3	35.08	104	0.270	2.556	2.550	4.111	13.003
	β-Cu2V2O7	24.54	200	0.272	3.625	3.600	7.249	09.640
$Al_{50}V_{20}Cu_{30}O$	α-Al_2O_3	35.04	104	0.282	2.558	2.552	4.110	13.032
	β-Cu2V2O7	43.20	-133	0.321	2.092	2.088	7.220	09.700

Furthermore, the decrease in crystallite size led to an increase in the dislocation density (δ), calculated using Equation (2) [6].

$$\boldsymbol{\delta} = \frac{1}{D^2} \qquad (2)$$

As summarized in Table 2, These results suggest that defects and vacancies became more prominent with the increasing molar concentration of copper.

Additionally, we examined the lattice constants (a, b, and c) for the dominant phases, α-Al_2O_3 and β-$Cu_2V_2O_7$, using equations (3) and (4) for hexagonal structures. The unit cell volume (V) and strain (ε) were calculated using equations (5) and (6), with the calculated values provided in Table 2. The unit cell volume and strain for all samples and the lattice constants were in good agreement with others [7]. Notably, the lattice constant (a) decreased as the molar concentration of copper increased, a trend that can be attributed to the diminishing values of ionic radius and the consequent decrease in crystallite size.

$$\frac{1}{d^2} = \frac{h^2}{a^2} + \frac{k^2}{b^2} + \frac{l^2}{c^2} \qquad (3)$$

$$\frac{1}{d^2} = \frac{1}{\sin^2\beta}\left(\frac{h^2}{a^2} + \frac{k^2\sin^2\beta}{b^2} + \frac{l^2}{c^2} - \frac{2hl\cos\beta}{ac}\right) \qquad (4)$$

$$V = 0.866\, ca^2 \qquad (5)$$

$$\varepsilon = \frac{\beta\cos\theta}{4} \qquad (6)$$

This comprehensive analysis of structural properties sheds light on the intricate interplay of materials in these mixed oxide nanopowders and their impact on crystallinity and lattice characteristics.

Table 2 Structure properties of the α-Al_2O_3 / V_2O_5/CuO at different molar ratio of Al^{+3} and Cu^{+1}

Samples	Phase oxide	c/a	V (Å^3)	D (nm)	δ*10^15 (m)$^{-2}$	Strain (ε)
Pure α-Al_2O_3	α-Al_2O_3	2.73	254.51	43.10	5.38	0.046
Al_{80} $V_{20}Cu_{0.0}O$	α-Al_2O_3	3.16	191.13	34.84	8.24	0.057
Al_{70} $V_{20}Cu_{10}O$	α-Al_2O_3	3.16	190.66	31.79	0.99	0.063
	β-$Cu_2V_2O_7$	1.39	474.60	29.23	1.17	0.129
Al_{60} $V_{20}Cu_{20}O$	α-Al_2O_3	3.16	190.31	30.90	1.05	0.064
	β-$Cu_2V_2O_7$	1.33	438.68	29.88	1.12	0.066
Al_{50} $V_{20}Cu_{30}O$	α-Al_2O_3	3.17	190.64	29.54	1.15	0.067
	β-$Cu_2V_2O_7$	1.34	437.89	26.60	1.41	0.075

3.2. Optical properties

The optical properties of pure α-Al_2O_3 and (α-Al_2O_3)$_{80-x}$ (V_2O_7)$_2$(Cu_2O)$_x$ at x = (1%, 2%, and 3%) nanopowders, each with varying molar ratios, were meticulously examined. The transmittance spectra of these samples were measured across a wavelength range spanning from 200 nm to 800 nm. Notably, the transmittance levels were particularly high in the vicinity of 300 nm. However, beyond this wavelength, the transmittance values began to decline, as depicted in Figure 3. For instance, the ($Al_{80}V_{20}$Cu0.0) sample displayed a transmittance of approximately 90%. This relatively high transmittance could be attributed to the specific coloration characteristics of this particular sample. In contrast, as the molar concentration of copper increased in the ($Al_{70}V_{20}Cu_1$0) sample, the transmittance soared to approximately 95%, indicating improved light transmission. Continuing this trend, further increases in the molar concentration of copper in both the ($Al_{60}V_{20}Cu_{20}$) and ($Al_{50}V_{20}Cu_{30}$) samples resulted in transmittance levels of around 60% and 45%, respectively. This suggests a clear correlation

between the presence of copper and the optical properties of the mixed oxide nanopowders, with increased copper concentrations leading to enhanced transmittance.

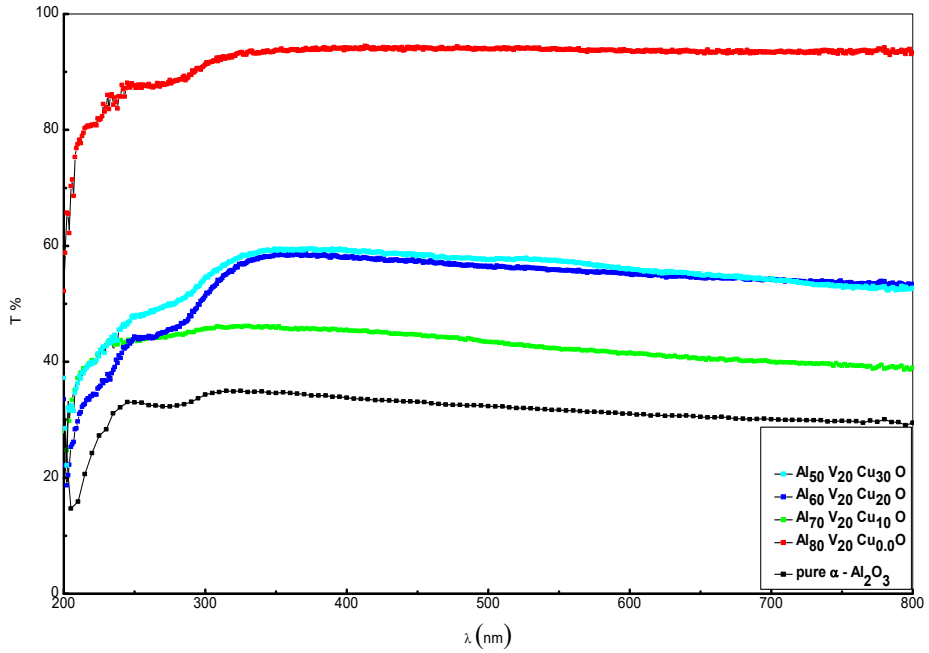

Fig 3 *UV spectra for transmittances with* wavelengths (λ nm) *for all samples.*

The determination of band energy in semiconductor materials is often facilitated through optical absorption studies. Figure 4 showcases the absorption characteristics of pure α-Al_2O_3, where it becomes evident that absorption intensifies with the increase in wavelength. Notably, the absorption edge of pure α-Al_2O_3 is pinpointed at approximately 280 nm, a finding that aligns with prior research [8]**.** Extending the investigation to the mixed oxide nanopowders, we observe the absorption spectra shown in Figure 4. In these spectra, distinct absorption edges become apparent for each sample, specifically at 331 nm, 344 nm, 364 nm, and 387.5 nm. These values correspond to the samples $Al_{80}V_{20}Cu_{0.0}O$, $Al_{70}V_{20}Cu_{10}O$, $Al_{60}V_{20}Cu_{20}O$, and $Al_{50}V_{20}Cu_{30}O$, respectively. These absorption edges are significant as they signify the photoexcitation of electrons from the valence band to the conduction band within the samples. Furthermore, the absorption bands are attributed to electronic transitions occurring from the

occupied 2p bands of oxygen to the unoccupied 3d bands of vanadium [9]. This optical absorption study offers valuable insights into the band energy characteristics of the mixed oxide nanopowders, shedding light on their semiconductor properties and potential applications.

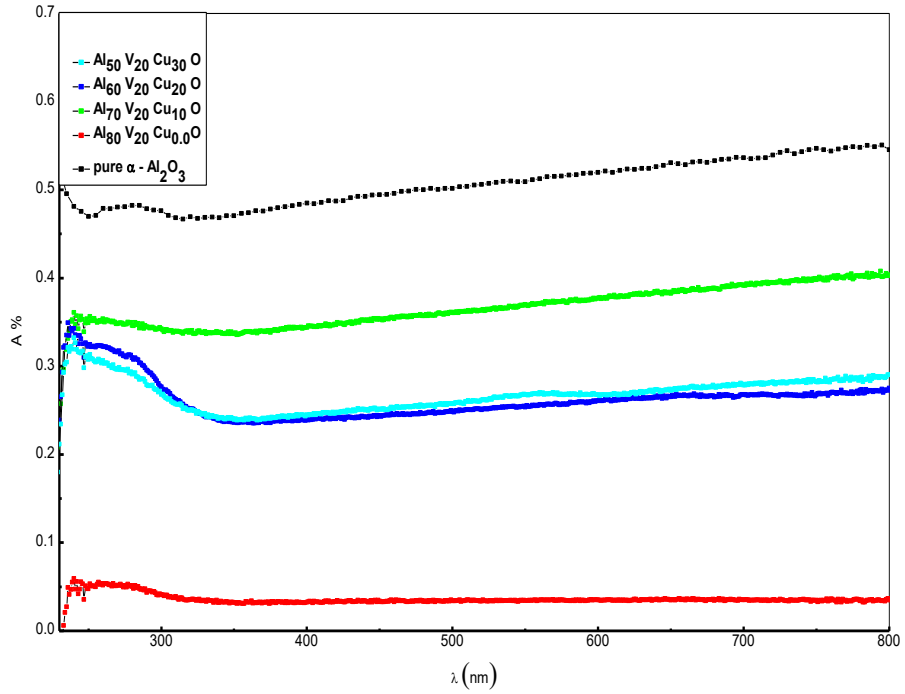

Fig 4 *The absorption of pure and with different concentrations.*

To provide deeper insights into the experimental data, we employed theoretical Equation (8) [16], to fit the observed results

$$\alpha h\nu = B(h\nu - E_g)^{\frac{1}{n}} \qquad (8)$$

Equation 8, which relates the absorption coefficient (α) to various parameters, such as Planck's constant (h), incident light frequency (v), a characteristic parameter (B), and the band gap energy (Eg), also incorporates the variable exponent (n). The quality of the fit was found to be optimal when n was set to 2, suggesting that the transitions observed are directly allowed.

The band gap energy (Eg) was determined for all the samples, including pure α-Al_2O_3 and (α-Al_2O_3)$_{80-x}$(V_2O_7)$_{20}$(Cu_2O)$_x$ at x = (1%, 2%, and

3%). The obtained band gap values were as follows: 5.21 eV for pure α-Al_2O_3, and 3.62 eV, 3.44 eV, 3.38 eV, and 3.28 eV for the respective mixed oxide nanopowders. Notably, the band gap value of 5.21 eV for pure α-Al_2O_3 closely aligns with prior research, confirming the reliability of the measurement, as shown in Figure 5.

Furthermore, an interesting trend emerged when examining the impact of varying the concentration of aluminum oxide and copper within the nanopowders. With a reduction in the concentration of Al2O3 and a simultaneous increase in the molar concentration of copper, the band gap of the nanopowders decreased. This trend is visually depicted in Figure 6 and quantitatively summarized in Table 3. The decrease in the band gap energy holds significance for potential applications, as it implies changes in the electronic properties of these materials, further expanding their utility in various technological and scientific domains.

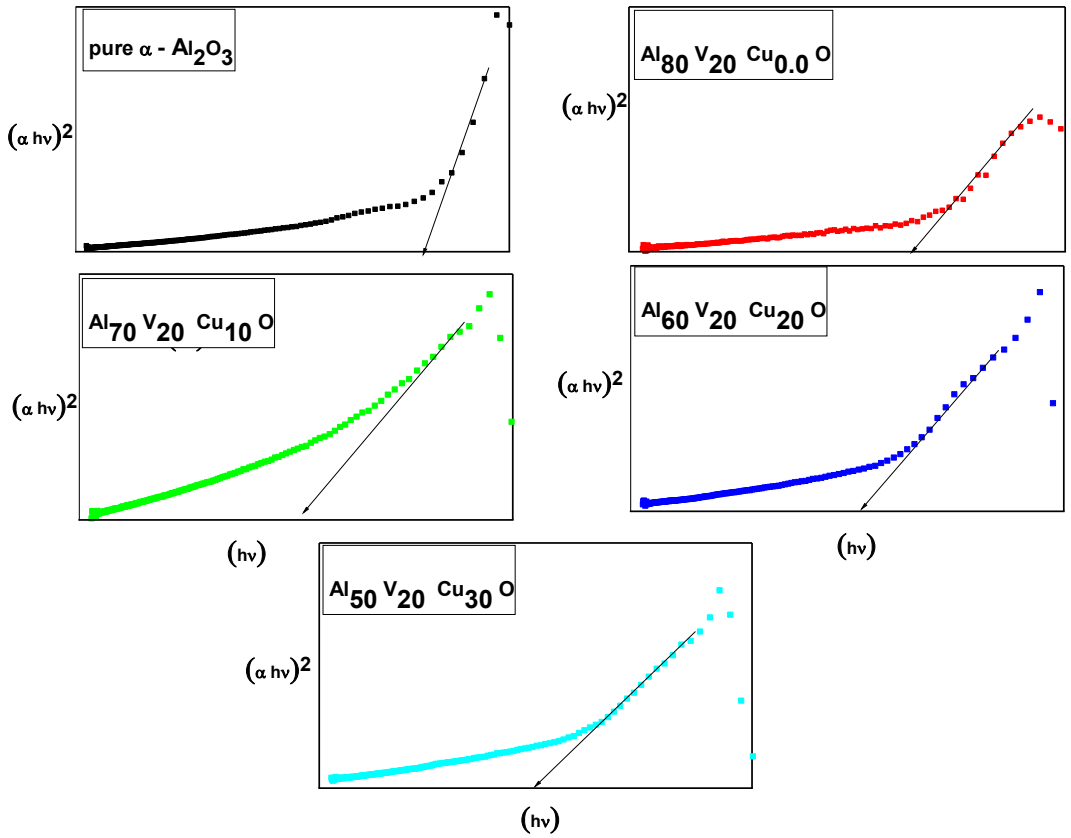

Fig 5 *Plots of the $(\alpha hv)^2$ versus the photon energy (hv) of the pure and with Cu % nanopowders for all samples.*

The reduction in the band gap value observed can be attributed to the emergence of empty levels induced by defects situated within the band gap. This phenomenon is well-documented, where the band gap of any material is intricately controlled by the concentration of defects it harbors. In the case of α-Al2O3, two types of defects play pivotal roles: donor defects, represented by oxygen vacancies, and acceptor defects, which are denoted as Al interstitials. These defects introduce energy levels situated below the conduction band and above the valence band, respectively. The genesis of these energy levels can be traced back to two fundamental reactions. Firstly, the Al interstitial defects are the result of the Frenkel reaction, a process where an atom is displaced from its original lattice site and occupies an interstitial position within the crystal structure. On the other hand, oxygen vacancy defects emerge from the Schottky reaction, which involves the simultaneous creation of vacancies for both cations and anions within the crystal lattice [10].

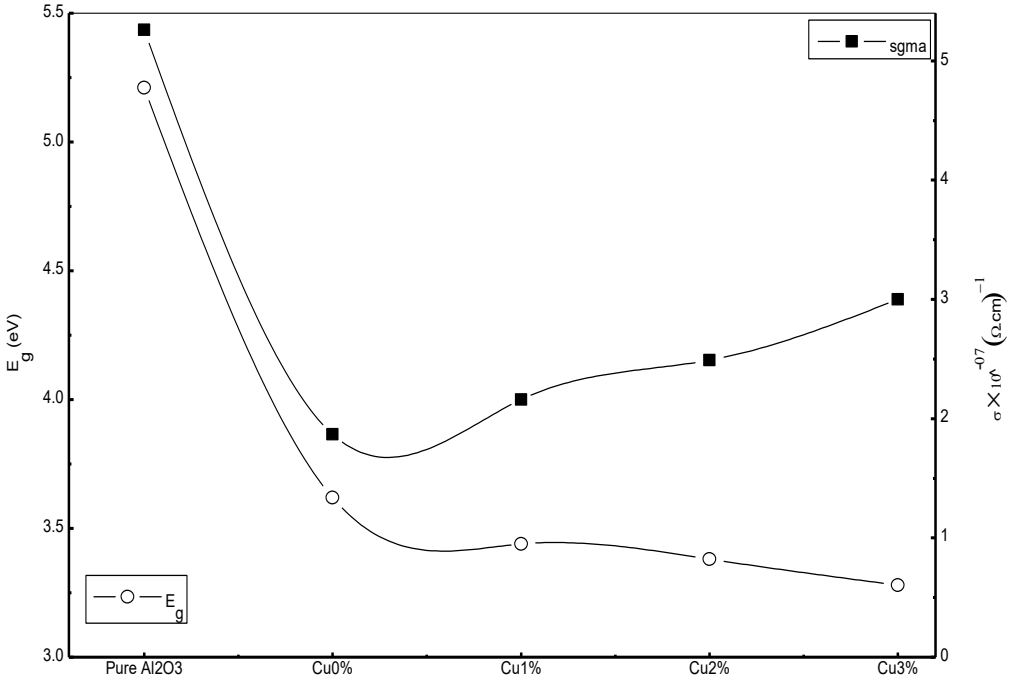

Fig 6 *Variation of both the energy gap (E_g) and electrical conductivity(σ)at α-Al_2O_3 and Cu (1,2, and 3 %).*

The presence and concentration of these defects and their intricate interplay fundamentally influence the band gap of the material. This understanding of defect-induced alterations in the band gap offers valuable insights into the electronic properties of the mixed oxide nanopowders, providing a foundation for the exploration of their potential applications in various scientific and technological contexts.

3.3. Electrical properties

The electrical properties of the materials were further assessed by measuring the current-voltage (I-V) characteristics and determining the ohmic resistance (R) for both pure α-Al_2O_3 and $(\alpha\text{-}Al_2O_3)_{80-x}(V_2O_7)_{20}(Cu_2)_x$ at x=(1%, 2%, and 3%) nanopowders, each with distinct molar ratios. The results unveiled a clear trend in the ohmic resistance, where it consistently decreased with the progressive increase in the molar concentration of copper, as detailed in Table 3. This decrease in ohmic resistance signifies a corresponding increase in electrical conductivity (σ), a trend visually presented in Figure 6. The σ can be expressed as a function of the R, based on the σ = L/A×(1/R), with units in (Ω cm)^-1. The variation in electrical conductivity is governed by the changing ohmic resistance, where a decrease in resistance leads to enhanced conductivity. A pivotal aspect to consider is that the σ within the sample is influenced by multiple factors. One of these factors is the movement of free electrons, a phenomenon closely associated with the presence of copper within the material [11]. The introduction of copper facilitates and eases the movement of free electrons, consequently resulting in higher electrical conductivity [12].

This observation highlights the profound influence of the molar concentration of copper on the electrical properties of the mixed oxide nanopowders. It signifies the potential for tailored electrical characteristics in these materials, which can be harnessed for specific applications requiring controlled conductivity and electrical behavior.

Table 3 Optical energy gap and electrical conductivity of pure α-Al_2O_3 and mixed oxide**.**

Samples	E_g (eV)	R (kΩ)	σ $(\Omega.cm)^{-1}$
Pure α-Al_2O_3	5.21	28.6 E^{9}	5.26 E^{-12}
Al_{80} $V_{20}Cu_{0.0}O$	3.62	769.3	1.87 E^{-07}
Al_{70} $V_{20}Cu_{10}O$	3.44	666.7	2.16 E^{-07}
Al_{60} $V_{20}Cu_{20}O$	3.38	579.8	2.49 E^{-07}
Al_{50} $V_{20}Cu_{30}O$	3.28	479.2	3.00 E^{-07}

The obtained electrical conductivity (σ) values in this study fall within the conventional range typically associated with semiconductors, which typically spans from 10^4 to 10^9 $\Omega^{-1}.cm^{-1}$ [13]. Notably, these findings are consistent with established values for α-Al_2O_3, which typically exhibits an average electrical conductivity of (6.87×10^{-12} ± 1.22×10^{-14} $\Omega^{-1}.cm^{-1}$) [14]. This alignment underscores the reliability and validity of the measurements. Furthermore, the electrical conductivity values obtained for the mixed oxide nanopowders, particularly for CuO and V_2O_5, also bear similarity to well-documented values in the literature. For instance, CuO exhibits electrical conductivity ranging between (1.1×10^{-4} and 2.77×10^{-4} $\Omega^{-1}.cm^{-1}$) [15]. While V_2O_5 typically displays electrical conductivity in the range of (2.53×10^{-4} $\Omega^{-1}.cm^{-1}$) [16]. This consistency in the electrical conductivity values between the experimental findings and established values can be attributed, in part, to the ionic radii of aluminum (Al) and copper (Cu) present within the structural properties of the materials. The interaction and distribution of these elements within the material play a pivotal role in enhancing electrical conductivity [17]. These results provide valuable insights into the underlying mechanisms governing the electrical properties of the mixed oxide nanopowders, offering opportunities for applications that require controlled and predictable electrical behavior.

4. Conclusions

In this study, we successfully synthesized both pure α-Al_2O_3 and $(\alpha\text{-}Al_2O_3)_{8-x}(V_2O_7)_{20}(Cu_2O)_x$ at x=(1%, 2%, and 3%) nanopowders, employing the sol-gel method, followed by heat treatment at 200 °C for 5 hours. The comprehensive examination of these materials yielded several noteworthy findings. XRD analyses demonstrated the high crystallinity of all samples, providing evidence of their well-defined structural characteristics. Notably, the crystallite size was accurately calculated using the Scherrer formula. For pure α-Al_2O_3, the crystallite size was determined to be 43.10 nm, consistent with its hexagonal structure. In contrast, for $(\alpha\text{-}Al_2O_3)_{80-x}(V_2O_7)_{20}(Cu_2O)_x$ in the mixed oxide nanopowders, the crystallite size exhibited variation, falling within the range of 34.84 nm to 29.54 nm. The band gap values for these materials also showed variation, ranging from 5.21 eV to 3.28 eV, indicative of the materials' semiconductor properties. Furthermore, the electrical conductivity exhibited a notable trend, with the resistance progressively decreasing as the molar concentration of copper increased. These findings collectively underline the potential and versatility of these mixed oxide nanopowders, particularly in applications that benefit from controlled crystallinity, tunable band gap characteristics, and regulated electrical conductivity.

Acknowledgment

The authors gratefully acknowledge to Mr. Ahmed Al-Khalki .

References

[1] M.A.A. Al-Mushaki, S.A. Al-Ariki, A. Alnehia, Effect of copper oxide (CuO) and vanadium oxide (V2O5) addition on the structural, optical and electrical properties of corundum (α-Al2O3), Sci. Rep. 13 (2023) 16100. https://doi.org/10.1038/s41598-023-43309-1.

[2] W. Shaheen, I.H. Abd El Maksod, Thermal characterization of individual and mixed basic copper carbonate and ammonium metavanadate systems, Journal of alloys and compounds 476 (2009) 366-372.

[3] A. Lashgari, S. Ghamami, M. Golzani, G. Salgado-Morán, L. Mendoza-Huizar, P.M. Romero, Biocidal activity of CuO nanoleaves against AGS cells, S. Aureus, E. Coli, and Micrococcus, Afinidad 75 (2018).

[4] D. Volanti, D. Keyson, L. Cavalcante, A.Z. Simões, M. Joya, E. Longo, J.A. Varela, P. Pizani, A. Souza, Synthesis and characterization of CuO flower-

nanostructure processing by a domestic hydrothermal microwave, Journal of Alloys and Compounds 459 (2008) 537-542.

[5] K. Chitrarasu, J.U. Bhanu, R. Dhanabal, A. Chandrabose, P. Thangadurai, Structural evolution and electrical properties of the biphasic compound α-Al2O3: MgAl2O4, Materials Research Bulletin 90 (2017) 244-252.

[6] . S. Al Ariki, Yahya, N.A.A., Al-Ansi, S.A. et al. Synthesis and comparative 22

study on the structural and optical properties of ZnO doped with Ni and Ag 23

nanopowders fabricated by sol gel technique. Sci Rep 11, 11948 (2021). 24

https://doi.org/10.1038/s41598-021-91439-1.

[7] S.P. Patil, L. Jadhav, D.P. Dubal, V. Puri, Characterization of NiO–Al2O3 composite and its conductivity in biogas for solid oxide fuel cell, Materials Science-Poland 34 (2016) 266-274.

[8] P. Prashanth, R. Raveendra, R. Hari Krishna, S. Ananda, N. Bhagya, B. Nagabhushana, K. Lingaraju, H. Raja Naika, Synthesis, characterizations, antibacterial and photoluminescence studies of solution combustion-derived α-Al2O3 nanoparticles, Journal of Asian Ceramic Societies 3 (2015) 345-351.

[9] R. Suresh, K. Giribabu, R. Manigandan, S. Munusamy, S.P. Kumar, S. Muthamizh, A. Stephen, V. Narayanan, Doping of Co into V2O5 nanoparticles enhances photodegradation of methylene blue, Journal of Alloys and Compounds 598 (2014) 151-160.

[10] N. Bajaj, S. Omanwar, Low-temperature stearic acid sol–gel synthesis of α-Al 2 O 3 quantum dots and its optical properties, Journal of Sol-Gel Science and Technology 75 (2015) 1-5.

[11] V. Rajkovic, D. Bozic, M.T. Jovanovic, Effects of copper and Al2O3 particles on characteristics of Cu–Al2O3 composites, Materials & Design 31 (2010) 1962-1970.

[12] A. Sadoun, M. Mohammed, E. Elsayed, A. Meselhy, O.A. El-Kady, Effect of nano Al2O3 coated Ag addition on the corrosion resistance and electrochemical behavior of Cu-Al2O3 nanocomposites, Journal of Materials Research and Technology (2020).

[13] S.C. Das, Characterization of structural, optical and electrical properties of Ni doped ZnO thin films, (2012).

[14] I. Momohjimoh, N. Saheb, M. Hussein, T. Laoui, N. Al-Aqeeli, Electrical conductivity of spark plasma sintered Al2O3–SiC and Al2O3-carbon nanotube nanocomposites, Ceramics International (2020).

[15] V.S. de Souza, H.O. da Frota, E.A. Sanches, Polyaniline-CuO hybrid nanocomposite with enhanced electrical conductivity, Journal of Molecular Structure 1153 (2018) 20-27.

[16] R. Barde, S. Waghuley, dc Electrical conductivity of V2O5-P2O5 binary glassy systems, J. Phys.: Conference Series, 2012, pp. 012019.

[17] S. Islam, G. Lakshmi, A.M. Siddiqui, M. Husain, M. Zulfequar, Synthesis, electrical conductivity, and dielectric behavior of polyaniline/V2O5 composites, International Journal of Polymer Science 2013 (2013).

****

ISSN:2617-4294

The Scientific Journal Of The Faculty Of Education

Referreed, Bi-annual Journal - Issued by Faculty of Education, Thamar University